Distinction between Pore Assembly by Staphylococcal α-Toxin versus Leukotoxins

Olivier R. Joubert, Joëlle Voegelin, Valérie Guillet, Samuel Tranier, Sandra Werner, Didier A Colin, Mauro Dalla Serra, Daniel Keller, Henri Monteil, Lionel Mourey, et al.

Hindawi Publishing Corporation
Journal of Biomedicine and Biotechnology
Volume 2007, Article ID 25935, 13 pages
doi:10.1155/2007/25935

Research Article

Distinction between Pore Assembly by Staphylococcal α-Toxin versus Leukotoxins

Olivier Joubert,[1] Joëlle Voegelin,[1] Valérie Guillet,[2] Samuel Tranier,[2] Sandra Werner,[3] Didier A. Colin,[1] Mauro Dalla Serra,[4] Daniel Keller,[1] Henri Monteil,[1] Lionel Mourey,[2] and Gilles Prévost[1]

[1] *Laboratoire de Physiopathologie et d'Antibiologie des Infections Bactériennes Emergentes et Nosocomiales, EA 3432, Institut de Bactériologie de la Faculté de Médecine, Université Louis Pasteur-Hôpitaux Universitaires de Strasbourg, 3 Rue Koeberlé, 67000 Strasbourg, France*
[2] *Groupe de Biophysique Structurale, Département Mécanismes Moléculaires des Infections Mycobactériennes, Institut de Pharmacologie et de Biologie Structurale (IPBS), CNRS-UMR 5089, 205 Route de Narbonne, 31077 Toulouse Cedex, France*
[3] *Société Parogène, Faculté de Médecine et d'Odontologie, Université Louis Pasteur-Hôpitaux Universitaires de Strasbourg, 11 Rue Humann, 67085 Strasbourg Cedex, France*
[4] *Istituto di BioFisica (IBF), Consiglio Nazionale delle Richerche (CNR), Via Sommarive 18, 38050 Povo, Trento, Italy*

Received 10 August 2006; Revised 7 November 2006; Accepted 6 December 2006

Recommended by Shahid Jameel

The staphylococcal bipartite leukotoxins and the homoheptameric α-toxin belong to the same family of β-barrel pore-forming toxins despite slight differences. In the α-toxin pore, the N-terminal extremity of each protomer interacts as a deployed latch with two consecutive protomers in the vicinity of the pore lumen. N-terminal extremities of leukotoxins as seen in their three-dimensional structures are heterogeneous in length and take part in the β-sandwich core of soluble monomers. Hence, the interaction of these N-terminal extremities within structures of adjacent monomers is questionable. We show here that modifications of their N-termini by two different processes, using fusion with glutathione S-transferase (GST) and bridging of the N-terminal extremity to the adjacent β-sheet via disulphide bridges, are not deleterious for biological activity. Therefore, bipartite leukotoxins do not need a large extension of their N-terminal extremities to form functional pores, thus illustrating a microheterogeneity of the structural organizations between bipartite leukotoxins and α-toxin.

1. INTRODUCTION

Staphylococcal bipartite leukotoxins and α-toxin belong to a single family of structurally related β-stranded pore-forming toxins (Figure 1). Leukotoxins are constituted by a class S protein (32 kd) that binds to the surface of target cells prior to a class F protein (34 kd) distinct in sequence [1]. Then, these proteins oligomerise to octamers or hexamers [2–5], induce Ca^{2+}-activation [6], and form monovalent cation-selective β-barrel transmembrane pores [7]. Each protomer contributes to the pore by transforming a central β-sheet domain into a β-hairpin [8, 9]. Five loci encoding leukotoxins are characterized [9]. Several of these loci, encoding the Panton-Valentine leucocidin (PVL), gamma-hemolysin, [10] and LukE-LukD [11], may be present together and are expressed in a single isolate. The S and F components can then combine to give a specific leukotoxin. However, they do not combine with α-toxin, also present in almost all isolates, for an action onto natural target cells [12], that is, human polymorphonuclear cells or erythrocytes. Panton-Valentine leucocidin, which is composed of LukS-PV and LukF-PV, is associated with furuncles [13] and pneumonia [14]. Bipartite leukotoxins show a complementary spectrum for lytic functions towards human blood cells including lymphocytes and erythrocytes, accounting for the bacterial virulence. Furthermore, leukotoxins and α-toxin differ from each other by the respective cationic and anionic selectivities of their pores [6, 15, 16].

X-ray diffraction and other techniques have been used to study the heptameric pore of α-toxin [17–21]. The crystal structure of the assembled α-toxin [20] revealed that the transmembrane β-barrel that forms the pore corresponds

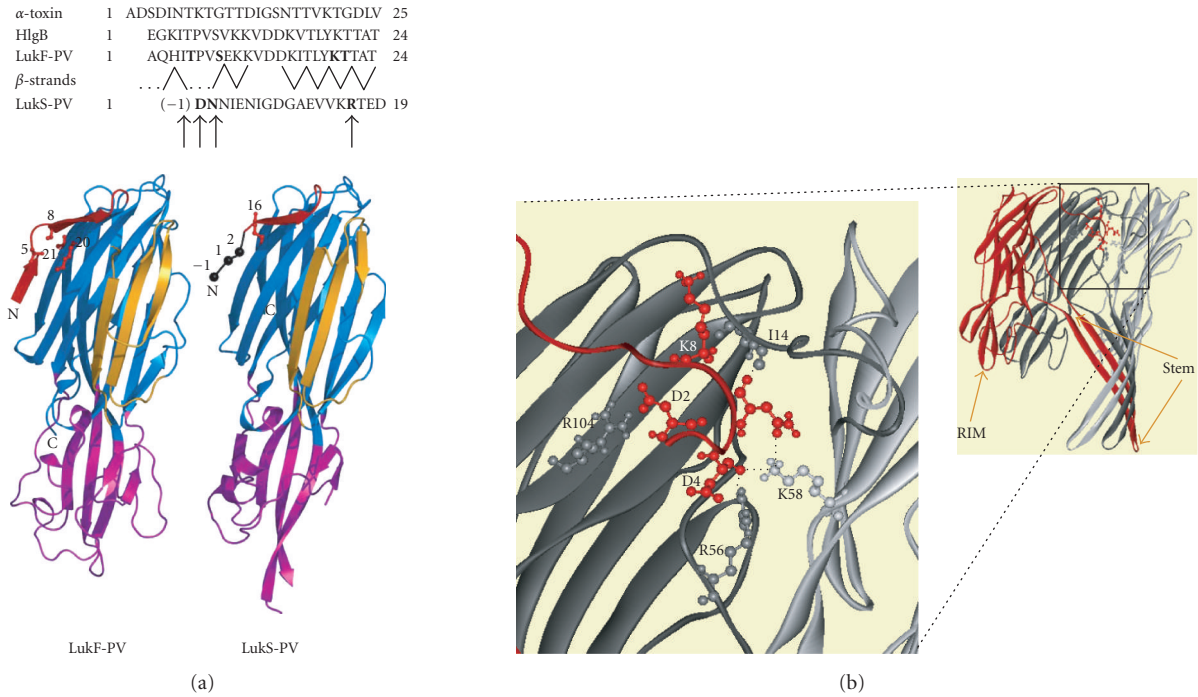

FIGURE 1: Structural features of the N-terminal extremities of staphylococcal bipartite leukotoxins and α-toxin. (a) Sequence alignment of the N-termini of staphylococcal α-toxin and of the two components LukF-PV and LukS-PV of the Panton-Valentine leucocidin. The strands arrangement of LukF-PV is indicated by dashes. Cysteine-substituted residues, indicated in bold in the sequences, are also shown on the 3D structures of LukF-PV (PDB code 1pvl) and LukS-PV (PDB code 1t5r). (b) For comparison, view three protomers of the α-toxin heptamer (PDB code 7AHL) and polar interactions involving the N-terminal extremity of a given subunit (red) with residues of two adjacent protomers (grey and dark grey) within the α-toxin pore lumen.

to the stem domain of a mushroom-shaped structure. It also revealed that the N-terminal extremity, also called the amino latch, of each protomer interacts with two adjacent protomers in the mouth of the pore lumen. The 3D structures of the soluble form of two F monomers, LukF-PV from the Panton-Valentine leucocidin (Figure 1(a)) [8] and HlgB from gamma-hemolysin [22], have also been determined. They showed that the central stem domain is prefolded as three β-strands stacked to the core of the soluble proteins. This core is formed of a β-sandwich to which the N-terminal extremity of the soluble F proteins contributes to one strand. Despite the high similarity between the F and S structures, the N-terminal extremity of LukS-PV appeared shorter [23]. The F and S proteins must undergo a number of conformational modifications during oligomerization and β-barrel formation to evolve to a functional transmembrane pore [24, 25].

Since the possible unfolding of the N-terminal extremity to interact with adjacent subunits is unclear, and that modifying the N-termini for bioengineering purposes could considerably influence their function, we report that some biological activity is retained by recombinant proteins after glutathione S-transferase (GST) fusion and expression in *Escherichia coli*. We also constrained this portion of the proteins to the β-sandwich by engineering disulfide bonds, and investigated the residual functions of new leukotoxins in order to verify if N-terminal extremities of leukotoxins must explore a large conformational space for their pore-forming activity.

2. MATERIALS AND METHODS

2.1. Bacterial strains and vectors

Escherichia coli XL1 blue cells (*recA1 endA1 gyrA96 thi1 hsdR17 supE44 relA1 lac* (F' *proAB lacI*^{q}*Z*ΔM15 *Tn*10 (*tet*^{r}))) (Stratagene, Amsterdam, The Netherlands) were used as recipient cells for transformation with recombinant pGEX-6P-1 following site-directed mutagenesis. *E. coli* BL21 (F$^-$, *ompT*, *hsdS* (*rB*$^-$, *mB*$^-$), *gal*) was used for overexpression of the glutathione-S-transferase (GST)—leukotoxin fusion genes, according to Manufacturer's instructions (Ge Healthcare, USA) [24].

2.2. Choice, construction, and purification of modified proteins

We considered alignment of N-terminal LukS-PV and LukF-PV sequence alignment extracted from the alignment of entire sequences (Figure 1(a)) [23]. We chose two pairs of LukF-PV amino acids, T5 and T21, and S8 and K20 for cysteine substitutions due to their respective close locations in the structure (Figure 1(a)) [8]. The distance between Cβ atoms of T5 and T21 (5.7 Å) and angles between thiol groups may allow the formation of disulfide bonds that would bridge

the first two β-strands of the protein (SSBond software, [26]). The other pair of amino acids seemed even more favorable for disulphide bridge formation, with a distance between Cβ atoms of 4.1 Å.

The situation was less obvious for LukS-PV, which has no counterpart to LukF-PV T5 (Figure 1(a)). Furthermore, the first three amino acids of the shorter LukS-PV N-terminal extremity could not be traced in the crystal structures of either wild type [23] or recombinant protein (unpublished results). Therefore, this N-terminal extremity may be poorly structured. To allow bridging with R16, which can be aligned with T21 of LukF-PV, we finally chose to substitute either LukS-PV N2 or D1 by a cysteine, and to introduce another cysteine residue upstream from D1 (called LukS-PV-1C) (Figure 1(a)).

Open reading frames corresponding to the secreted LukF-PV and LukS-PV encoding genes were previously cloned into the pGEX-6P-1 expression vector [24]. We further obtained five double mutants, LukS-PV(-1C)-R16C, D1C-R16C, N2C-R16C and LukF-PV T5C-T21C, S8C-K20C, using dedicated oligonucleotides in a two-step mutagenesis procedure similar to that of Quick Change mutagenesis (Stratagene, Calif., USA), except that *Pfu* Turbo DNA polymerase was replaced by Arrow *Taq* DNA polymerase, and T4 GP32 protein (Qbiogene Inc., Calif, USA).

GST∼LukS-PV and GST∼LukF-PV fusion proteins were purified for functional analysis by chromatography on glutathione-sepharose 4B followed by hydrophobic interaction chromatography (HIC, alkyl-superose, i.e., resource ISO—Ge Healthcare, USA). GST∼LukS-PV and GST∼LukF-PV eluted at 0.73 M and 0.78 M $(NH_4)_2SO_4$, respectively. All double cysteine-mutated proteins were purified by affinity chromatography on glutathione-sepharose 4B followed by cation-exchange FPLC chromatography (CEC) using an NaCl gradient from 0.05 M to 0.7 M [24]. The GST-tag was removed thanks to the PreScission protease. Nevertheless, it remains an octapeptide at the N-terminus which does not hamper the biological activities of the toxins [8, 24] (Amersham Biosciences). Hydrophobic interaction chromatography (HIC) was further applied using an $(NH_4)_2SO_4$ gradient from 1.3 M to 0.5 M to improve purifications. LukS-PV mutants eluted at 0.15 M NaCl and 1.02 M $(NH_4)_2SO_4$, whereas those of LukF-PV eluted at 0.1 M NaCl and 0.95 M $(NH_4)_2SO_4$. To avoid any disulfide links formation between free sulfhydryl groups of the cysteine residues of the fusion proteins and the GSH, all buffers used for the CEC and the HIC contain 1 mM DTT (except for GST fusion proteins). Controls for homogeneity were performed using SDS-PAGE, and the proteins were then stored at −80°C. We labelled two fully functional mutants, LukF-PV S27C and LukS-PV G10C, with fluorescein 5-maleimide (Molecular Probes, Leiden, The Netherlands) [24].

2.2.1. Oxidation and accessible thiol-titration

The cysteine mutants were first reduced with 10 mM DTT, before treating with $CuSO_4$, 1,10-phenanthroline (Sigma, USA). Briefly, proteins at a concentration of 20 μM were dialysed in 50 mM Hepes, 0.5 M NaCl, 10 mM DTT pH 7.5, and further equilibrated against 50 mM Hepes, 0.5 M NaCl, pH 7.5 to undergo oxidation. Proteins were then adjusted to 2 mL (20 μM) of the same buffer complemented with 1.5 mM $CuSO_4$, 5 mM 1,10-phenanthroline and incubated for 2 hours at 4°C. Protein solutions were then equilibrated against 50 mM Hepes, 0.5 M NaCl, 1 mM EDTA-Na_2, pH 7.5, and could then be frozen without loss of disulfide bonds and biological activity.

For the titration of free thiols, proteins were precipitated in 5% (w/v) trichloroacetic acid and left for 5 minutes at 0°C, pelleted by centrifugation and washed three times with the same solution. The precipitate was dissolved in 400 μL of N_2-saturated 0.2 M Hepes, 0.2 M NaCl, 1 mM EDTA-Na_2, 2% (w/v) SDS, pH 8.0. The remaining precipitated material (< 10% of total proteins) was removed by centrifugation and 300 μL of the supernatant was added to 30 μL of 10 mM 5-5′-di-thio-bis (2-nitro) benzoic acid (DTNB) ($\varepsilon = 13,600\ M^{-1}\cdot cm^{-1}$). After 10 minutes of reaction at room temperature, the amount of titrated thiols was estimated by OD at 412 nm and the molarity was compared to the protein concentration determined by the Lowry method.

2.3. Human polymorphonuclear cells (PMNs) and flow cytometry measurements

Human PMNs from healthy donors were purified from buffy coats as previously reported [27], and suspended at 5×10^5 cells/mL in 10 mM Hepes, 140 mM NaCl, 5 mM KCl, 10 mM glucose, 0.1 mM EGTA pH 7.3. Flow cytometry measurements from 3000 PMNs were carried out using a FacSort flow cytometer (Becton-Dickinson, Le Pont de Claix, France) equipped with an argon laser tuned to 488 nm [28]. We evaluated the intracellular calcium using flow cytometry of cells previously loaded with 5 μM Fluo-3 (molecular probes) in the presence of 1.1 mM extracellular Ca^{2+} by measuring the increase of Fluo-3 fluorescence. Pore formation and monovalent cation influx were revealed by the penetration of ethidium through the pores; cells were incubated 30 minutes with 4 μM ethidium prior to the addition of toxins in the absence of extracellular Ca^{2+} [24, 28]. Fluo-3 and ethidium fluorescence were measured using Cell Quest Pro software (Becton, Dickinson and Company). The results from at least four different donors were averaged and expressed as percentages of a control of human PMNs treated with the wild-type (WT) PVL. Base level values were obtained for each series of data from a control without addition of toxin. These were systematically subtracted from the other assays. Standard deviations values never exceeded 10% of the obtained values; they were removed from figures for clarity.

The dissociation constant ($k_{D[S]}$) of LukS-PV for the PMN membrane and that of LukF-PV for the PMN membrane-bound LukS-PV ($k_{D[F]}$) were previously reported to be 0.07 nM and 2.5 nM, respectively [29]. LukS-PV and mutants were applied at 1 nM while LukF-PV and derivatives were applied at 10 nM as an excess of toxins to their ligand(s). The binding properties of the modified proteins onto PMNs were estimated through competition experiments carried out in the absence of extracellular Ca^{2+}. Fluorescein-labelled

LukS-PV G10C (0.1 nM) and LukF-PV S27C (2 nM), and increasing concentrations of the respective mutants (from 1 to 1000 nM) were added 15 minutes before measuring the fluorescence retained at the surface of PMNs. For LukF-PV competitions, the PMNs were initially incubated for 10 minutes with 1 nM of LukS-PV. The IC_{50} value corresponds to the concentration of nonfluorescent competitor needed for 50% cell fluorescence inhibition, and is determined from the best fit of independent triplicates of the residual cell fluorescence [24]. The apparent inhibition constant, $k_{I\text{app}}$, was calculated from the following equation:

$$k_{I\text{app}} = \frac{IC_{50}}{\left(1 + [S^* \text{ or } F^*]/k_{D[S] \text{ or } [F]}\right)}, \quad (1)$$

where $[S^* \text{ or } F^*]$ are the concentrations of fluorescent LukS-PV or LukF-PV, and $k_{D[S] \text{ or } [F]}$ are the dissociation constants of LukS-PV (0.07 nM) or LukF-PV (2.5 nM).

2.4. Determination of pore radius

The pore formation induces a disruption in the cell membrane. It results in an increase of the cell size due to the difference of osmolarity between the cytoplasm and the medium. Indeed, the osmolarity is weaker in the medium than in the cytoplasm. The relative variations in PMN size were assessed by measuring of the forward light scatter (FSC) of cells (5×10^5 cells/ml) treated with WT or mutant 20 nM LukS-PV, WT or mutant 100 nM LukF-PV, and 30 mM PEG polymers (1000, 1500, 2000, 3000 Da) of different hydrodynamic radii (0.94, 1.12, 1.22, and 1.44 nm, resp.) [25]. FSC values were collected at 15 minutes after toxin application. If the sizes of the PEG molecules are similar or greater than the diameter of lumen, they cannot pass through the pores, and then cannot balance the osmolarity between both compartments. In that case, the FSC variations are weak. If the sizes of the PEG molecules are smaller than the diameter of lumen, they can pass through the pore with balancing the osmolarity between the two compartments. It results in a rise of the FSC variations.

2.5. Identification of oligomers

Denaturing polyacrylamide gel electrophoresis (SDS-PAGE) was carried out on oxidized leucotoxin-treated human PMNs. Preparations at 5×10^7 cells/mL in 10 mM Hepes, 140 mM NaCl, 5 mM KCl, 10 mM glucose, 0.1 mM EGTA, pH 7.3, were incubated with 100 nM of LukS-PV and LukF-PV derivatives in the presence of 10 μL/mL of a mammalian cell-tissue antiprotease cocktail (Sigma, USA). After a 45-minute incubation at 22°C, the biological activity was assessed by optical microscopy, the cells were washed twice and then resuspended in 1 mL of the same buffer containing an antiprotease cocktail (1 μL/mL) as above. The cells were ground in a FastPrep apparatus (QBiogene, Bio101, Illkirch, France) using FastPrep Blue tubes for an orbital centrifugation (10 seconds, 3600 rpm, room temperature). The membranes were harvested by ultracentrifugation for 20 minutes at 20000 $\times g$ at 4°C. The membrane pellets were resuspended in 100 μL of the same buffer complemented with 2 μL of antiprotease cocktail containing 1% (w/v) saponin (Sigma), incubated for 30 minutes at room temperature and then centrifuged for 30 minutes at 22000 $\times g$. The supernatants were adjusted to 1 mM glutaraldehyde (in the above buffer) and incubated for 10 minutes at 50°C. One third volume of loading buffer (0.5 M Tris-HCl pH 8.5, 2% (w/v) SDS, 0.04% (w/v) bromophenol blue, 30% (v/v) glycerol) containing 100 mM ethanolamine to block the cross-linking reaction was added and assays were heated to 100°C for 5 minutes. Finally, 10 μL of the solution was loaded onto Tris-acetate, pH 8.1 polyacrylamide 3–8% (w/v) gels (Invitrogen, Calif, USA). Proteins were subjected to electrophoresis for 75 minutes at 150 V at room temperature in 50 mM Tris, 50 mM Tricine, pH 8.2, 0.1% (w/v) SDS, and then electroblotted onto nitrocellulose membranes for 1 hour at 30 V in 25 mM Tris, 192 mM glycine, pH 9.3, 20% methanol using a transfer Xcell II blot module (Invitrogen). The leukotoxins oligomers or components were characterized by immunoblotting using affinity-purified rabbit polyclonal antibodies and a peroxidase-labeled goat antirabbit antibody using ECL detection (Amersham Biosciences, Saclay, France) as previously described [24]. The apparent molecular masses were estimated from protein migration according to Precision Plus Protein Standards (Bio-Rad, USA).

3. RESULTS

3.1. GST-fusion proteins remain biologically active

GST∼LukS-PV and GST∼LukF-PV were purified to homogeneity and appeared as homogeneous proteins with apparent molecular masses of 57 and 60 kd, because of the fusion with the 26 kd GST (Figure 2(a)). The apparent binding of leukotoxin derivatives with cell membranes was assessed in competition with an increased amount of the functional fluorescein-labelled (∗) LukS-PV G10C* or LukF-PV S27C*. Apparent k_I of 0.039 nM was found for the WT LukS-PV binding to membranes and a value of 3.6 nM was found for the WT LukF-PV binding to LukS-PV-membrane complexes (data not shown). In these conditions, values of $k_{I\text{app}}$ determined for GST∼LukS-PV and GST∼LukF-PV (0.2 and 3.4 nM, resp.) remained close to the values obtained for the WT proteins. However, when GST∼LukF-PV was applied to the bound GST∼LukS-PV, a $k_{I\text{app}}$ of 17.6 nM was recorded, this marked difference may be due to some steric hindrance caused by GST molecules.

Combinations of LukS-PV with GST∼LukF-PV or of GST∼LukS-PV with LukF-PV led to Ca^{2+} induction in treated cells comparable to the WT proteins (Figure 2(b)). However, the combination of both fusion proteins required a longer time, *that is*, 4 minutes instead of 2 minutes, to reach a fluorescence maximum. Subsequent decrease of fluorescence is mainly due to the release of the fluorescent probe by pores and disrupted cell membranes.

The permeability to monovalent cations mediated by the pores was measured via the entry of ethidium and its combination with nucleic acids. Despite ethidium fluorescence being less sensitive than Ca^{2+} assay, these two influxes were

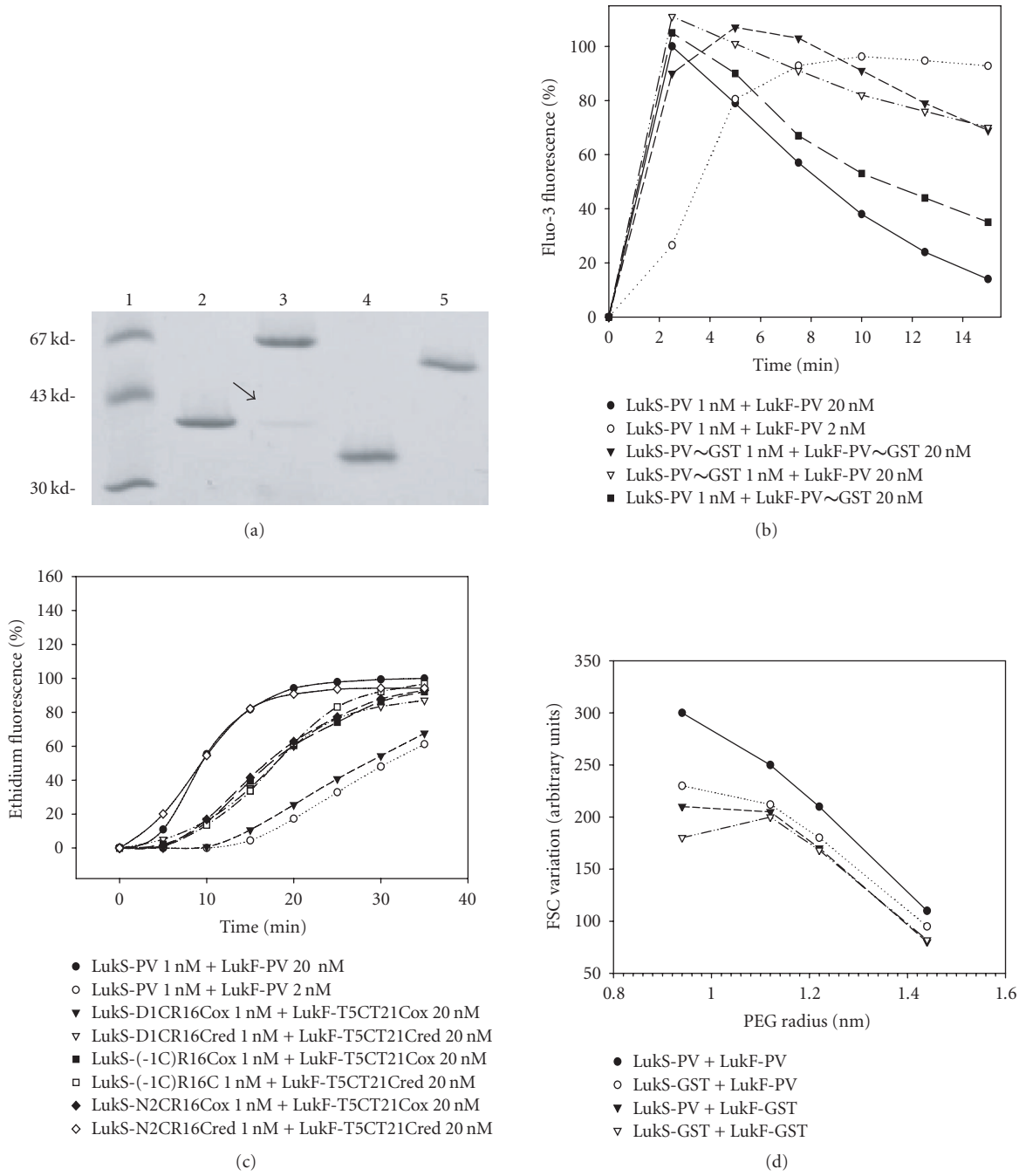

Figure 2: Biological activity of GST fusion proteins. (a) Control of homogeneity by 3%–8% (w/vol) SDS-PAGE of 200 ng of each purified protein is shown; (1) molecular ladder, (2) LukF-PV, (3) GST∼LukF-PV, (4) LukS-PV, (5) GST∼LukS-PV. (b) Flow cytometry evaluation of the Ca^{2+} entry into human PMNs mediated by combinations of wild-type LukS-PV and LukF-PV and GST fusion proteins. (c) Flow cytometry evaluation of the ethidium entry into human PMNs mediated by combinations of LukS-PV and LukF-PV and GST fusion proteins. (d) Hydrodynamic radius of pores formed by WT and fusion proteins in human PMNs determined after a 30-minute incubation of toxins (20 nM of S and 100 nM of F components). Osmotic protection by polyethylene glycol molecules was assessed by variations of the mean FSC (forward light scatter) value in the presence of PEG molecules of different hydrodynamic radii.

demonstrated to be independent [7, 24]. Fusion proteins tested alone did not generate entry of Ca^{2+} (not shown) and ethidium (Figure 2(c)). Ethidium entry showed a higher variation than what was observed for calcium, but the fusion proteins retained significant biological activity (Figure 2(c)). The activity of GST∼LukS-PV + LukF-PV lies between those obtained for PVL and for PVL with a 1 : 10 dilution of LukS-PV, whereas the activity of LukS-PV + GST∼LukF-PV was similar to that of PVL with the 1 : 10 dilution of LukS-PV (Figure 2(c)). The combination of both fusion proteins showed a considerably reduced ethidium influx, even if compared with the 1 : 10 dilution of LukS-PV (Figure 2(c)).

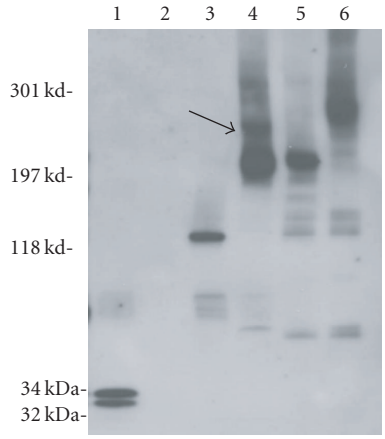

Figure 3: Oligomers formed by PVL and modified toxins. Oligomers were checked in solution or after recovery from treated human PMNs, 3–8% (w/v) SDS-PAGE and immunoblotting with anti-LukS-PV and anti-LukF-PV affinity-purified rabbit antibodies. Lane 1: LukS-PV + LukF-PV without membranes, lane 2: PMNs only, lane 3: GST∼LukS-PV + GST∼LukF-PV, lanes 4, 5, 6: toxins applied on PMNs membranes and then saponin/glutaraldehyde treated and heated 5 minutes at 100°C as described in materials and methods, lane 4: LukS-PV + GST∼LukF-PV, lane 5: GST∼LukS-PV + LukF-PV, lane 6: GST∼LukS-PV + GST∼LukF-PV.

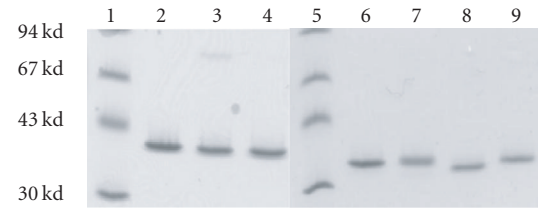

Figure 4: Control of homogeneity and absence of significant dimerization in nonreducing conditions by 3–8% (w/v) SDS-PAGE of 200 ng of each mutated protein: lane 1: molecular ladder, lane 2: LukF-PV, lane 3: LukF-PV T5C-T21C oxidized (ox), lane 4: LukF-PV S8C-K20Cox, lane 5: molecular ladder, lane 6: LukS-PV, lane 7: LukS-PV-1C-R16Cox, lane 8: LukS-PV D1C-R16Cox, lane 9: LukS-PV N2C-R16Cox.

This difference can again be explained by the steric hindrance caused by GST molecules. After osmotic protection with PEG molecules, all couples involving at least one fusion protein showed decays of the forward light scatter values comparable to those of the WT toxin (Figure 2(d)). The inflexion point calculated for each curve clearly indicated permeability to PEG molecules with a hydrodynamic radius cutoff between 1.12 and 1.2 nm. Thus, the diameter of the leukotoxin pores was not affected by GST fusion proteins [25].

We aimed at identifying oligomers formed by the fusion proteins (67 and 60 kd, resp.) within the human PMNs membranes to confirm the pore formation. When retrieved from cell membranes, we noticed that oligomers formed by LukS-PV and LukF-PV were very sensitive to detergents (saponin 1% and SDS 0.04%), as we only detected mixtures of monomers and dimers (Figure 3, lane 3). Therefore, we used a cross-linking agent, glutaraldehyde, applied consecutively after the saponin treatment, to help to stabilize the oligomers removed from the membranes in the presence of an excess of cell membrane proteins. Cross-linking proved efficient for both combination of fusion proteins (Figure 3, lanes 4–6), but essentially showed tetramers for all, in spite of the fact that hexamers might be suspected for the LukS-PV + GST∼LukF-PV combination (Figure 3, lane 4, see arrow). The use of anti-LukS-PV and anti-LukF-PV antibodies, alone or in combination, allowed the detection of similar high molecular mass oligomers containing GST fusion leukotoxins (data not shown). The materials were specific for the leukotoxins, since no immunoreactive product was observed when analyzing human PMNs alone (Figure 3, lane 2). The intensity of these bands rapidly decreased while the number of subunits increased. The increase of the steric hindrance due to the fusion GST proteins probably contributes to the intrinsic instability of leukotoxins pores when extracted from membranes and may impact the resolution of the complete oligomers (Figure 3, lanes 4–6). Therefore, we decided to characterize the oligomers for only WT proteins and double cysteine mutants (see below).

3.2. Integrity of double-cysteine mutants

Double-cysteine mutants were analyzed in their oxidized forms (Figure 4). Among the LukS-PV and LukF-PV double-cysteine mutants obtained in either reducing or oxidizing conditions, only oxidized LukS-PV N2C-R16C and oxidized LukF-PV T5C-T21C contained very small amounts of homodimers (< 8%). The presence of these dimers did not cause a significant loss of biological activity.

Once purified, proteins were kept in 10 mM DTT. After desalting, titration of accessible thiols with DTNB ranged from 85 to 97% of free thiols, depending on the mutants. After oxidation, accessible thiol residues in oxidized LukS-PV-1C-R16C, D1C-R16C, N2C-R16C, and LukF-PV T5C-T21C, S8C-K20C mutants decreased to less than 1.5% (1% was the limit of the titration assay). These mutants formed internal disulfide bonds (Figure 4, lanes 6 to 9).

3.3. Binding of double-mutated leukotoxins

Using similar conditions as for the fusion proteins, we determined the apparent binding constants of the different mutants to their respective ligands. For LukS-PV mutants, we found $k_{I\text{app}}$ values, ranging from 0.052 nM to 0.069 nM, similar to those of WT LukS-PV. Values for the binding of LukF-PV T5C-T21C to the LukS-PV mutants-membrane complexes ($k_{I\text{app}} = 2.8 - 5.2$ nM) were also close to that of the WT protein ($k_{I\text{app}} = 2.5$ nM). In contrast, binding of LukF-PV S8C-K20C was more affected. Indeed, binding of LukF-PV S8C-K20C to LukS-PV D1C-R16C and N2C-R16C gave $k_{I\text{app}}$ of 18.5 ± 2.5 and 12 ± 2 nM, respectively. Binding became even worse with LukS-PV and LukS-PV(-1C)-R16C with $k_{I\text{app}} = 37 \pm 5$ and 24 ± 6 nM, respectively.

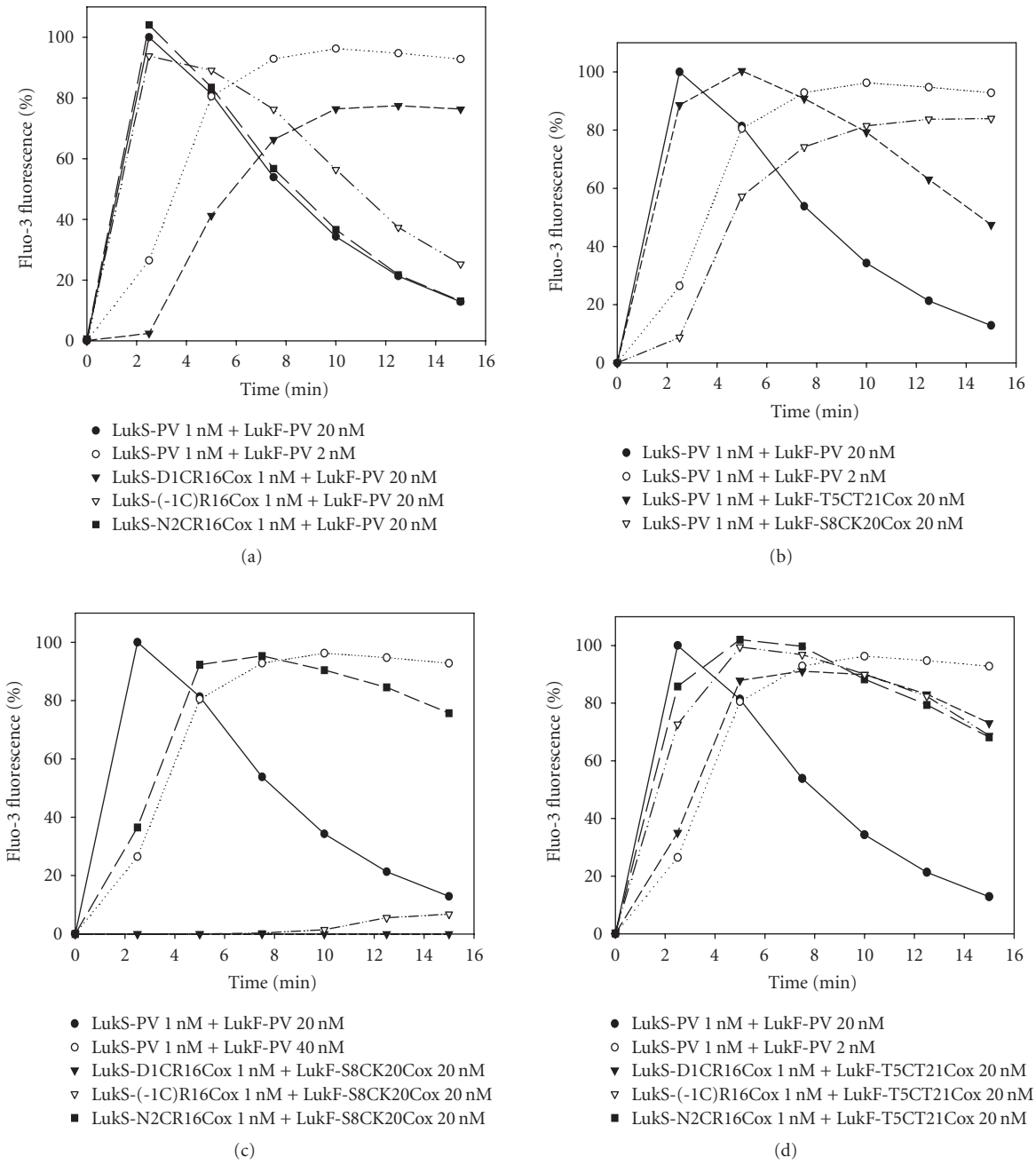

Figure 5: Flow cytometry evaluation of Ca^{2+} entry into human PMNs for different combinations of purified WT S and F proteins and their oxidized double mutants. (a) Oxidized LukS-PV mutants were tested with WT LukF-PV. (b) Oxidized LukF-PV double mutants were tested with WT LukS-PV. (c) Oxidized LukS-PV double mutants were tested with LukF-PV S8C-K20Cox. (d) Oxidized LukS-PV double mutants were tested with LukF-PV T5C-T21Cox.

3.4. Biological activities of the leukotoxin mutants

Ca^{2+} entry

Staali et al. [7] and Baba Moussa et al. [24] showed that Ca^{2+} influx and ethidium entry promoted by leukotoxins can be selectively inhibited. We evaluated the different oxidized LukS-PV and LukF-PV double mutants for their ability to activate PMNs and provoke Ca^{2+}-channel opening (Figure 5). In our system, we assayed LukS-PV at 0.1 or 1 nM in combination with LukF-PV at 2 or 20 nM, and compared activity of associations of LukS-PV proteins/mutants at 1 nM and LukF-PV proteins/mutants at 20 nM. Table 1 summarizes kinetics of cell-associated Ca^{2+} fluorescence for different combinations. When mutants were first combined with the heterologous WT protein, kinetics of Ca^{2+} influx comparable with that of the WT toxin were observed for combinations

Table 1: Times (min) to reach (a) 5% and (b) 100% of the Fluo-3 fluorescence characteristic of the cellular entry of Ca^{2+} due to calcium channels activation by combinations of PVL (taken as reference) and its mutants, n.r.: not reached, n.d.: not determined.

	LukF 40 nM	LukF 2 nM	LukF-T5CT21C	LukF-S8CK20C
LukS 1 nM	1.25[(a)] 2.5[(b)]	3.5[(a)] 10[(b)] (95%)	1.25[(a)] 5[(b)]	4.5[(a)] n.r.
LukS-D1CR16C	6[(a)] n.r.[(b)]	n.d.	3.4[(a)] 7.5[(b)] (90%)	n.r. n.r.
LukS-(-1C)R16C	1.25[(a)] 2.5[(b)]	n.d.	1.75[(a)] 5[(b)]	n.r. n.r.
LukS-N2CR16C	1.25[(a)] 2.5[(b)]	n.d.	1.5[(a)] 5[(b)]	3[(a)] 7.5[(b)] (95%)

involving LukS-PV(-1C)-R16C or N2C-R16C and LukF-PV at 20 nM (Figure 5(a)). In contrast, the kinetics for 1 nM LukS-PV D1C-R16C combined with LukF-PV was decreased to a lower value than that obtained for WT combination involving 2 nM of LukF-PV. The same was observed for LukS-PV + LukF-PV S8C-K20C, whereas the combinations involving LukF-PV T5C-T21C were almost as active as the WT toxin (Figure 5(b), Table 1). Greater variations in Ca^{2+} induction were obtained when associating oxidized mutants with each other (Figures 5(c) and 5(d)). Among the combinations involving LukF-PV S8C-K20C, only LukS-PV N2C-R16C significantly induced Ca^{2+} influx. The combinations of LukS-PV(-1C-R16C) and N2C-R16C with LukF-PV T5-T21C produced kinetics almost similar to the WT toxin, and the combination involving LukS-PV D1C-R16C showed a better Ca^{2+} influx than its combination with LukS-PV (Figures 5(a) and 5(d), Table 1). Altogether, these data indicate that constraining N-terminal extremities might not be detrimental to biological activity.

Ethidium entry induced by pore formation

Pore formation and ethidium entry promoted by the oxidized mutated proteins were more variable than Ca^{2+} entry (Figure 6). Table 2 summarizes kinetics of cell-associated ethidium fluorescence for different combinations. After combining with WT LukF-PV, LukS-PV N2C-R16C remained as active as WT LukS-PV, while LukS-PV(-1C)-R16C only retained 1 : 10 of activity (Figure 6(a), Table 2) and kinetics for LukS-PV D1C-R16C was dramatically affected. The kinetics of ethidium entry induced by LukS-PV combined with LukF-PV mutants was intermediate between those produced by a same concentration of LukF-PV and its 1 : 10 dilution. Combinations of reduced mutants with heterologous WT proteins or mutants did not show high difference in activity compared to the use of oxidized mutants (data not shown). Figures 6(c) and 6(d) show the results obtained for combinations of oxidized and reduced mutants. Except for LukS-PV(-1C)-R16C + LukF-PV T5C-T21C (Figure 6(c)), the associations of reduced mutants always induced higher ethidium influxes than those obtained with associations of oxidized mutants (Table 2). From combining oxidized mutants, the pairs involving LukS-PV(-1C)-R16C, N2C-R16C, combined with LukF-PV T5C-T21C showed intermediate activity (Table 2), while only LukS-PV N2C-R16C combined with LukF-PV S8C-K20C could be considered as significant as the last cited (Figure 6(d)). It has to be noticed that all combinations of oxidized mutants less prone to induce Ca^{2+} influx were also less effective in pore formation.

Pore radii

The pore radii of the most active oxidized leukotoxins were evaluated by osmotic protection induced with calibrated PEG molecules (Figure 7). PMNs were protected against osmotic disruption by PEG molecules having a hydrodynamic diameter between 1.12 nm and 1.22 nm. A same value ranging 1.2 nm was obtained for the WT toxin, indicating similar pore radii of these toxins.

3.5. Panton-Valentine leucocidin oligomers

Several experiments were carried out, checking for the recovery, the stability, and the occurrence of oligomers formed by PVL. Control of cells without PVL did not give evidence of cross-reacting material (Figure 8, lane 1). Challenging PVL oligomers with 4 ng of each component in solution was highly dependent on glutaraldehyde concentrations (Figure 8, lanes 3 and 4), while they show a little tendency to spontaneously form dimers (lane 2). Indeed, the use of 0.3 mM glutaraldehyde allowed to obtain various oligomers containing 2 to 10 units, at least, whereas 3 mM applied on these purified proteins dramatically affected signals (lane 4). Application of 30 ng of PVL per assay to PMNs only allowed observing few dimers in the described conditions without any glutaraldehyde treatment (Figure 8, lane 5). It has to be noticed that a nonboiled, but SDS-containing, assay resulted in insufficiently denatured materials, and even if treated by saponin and glutaraldehyde, this did not give interpretable results (Figure 8, lane 6). Saponin treatment of cells largely helped the release of protein-containing oligomers, despite the fact that saponin brought contaminating proteins (50% of the total bulk of proteins). Each assay on cells involve an original volume of 1 mL further concentrated to 100 μL. Cells treated with PVL, saponin, and with a consecutive cross-linking with 3% (v/v) glutaraldehyde allowed to

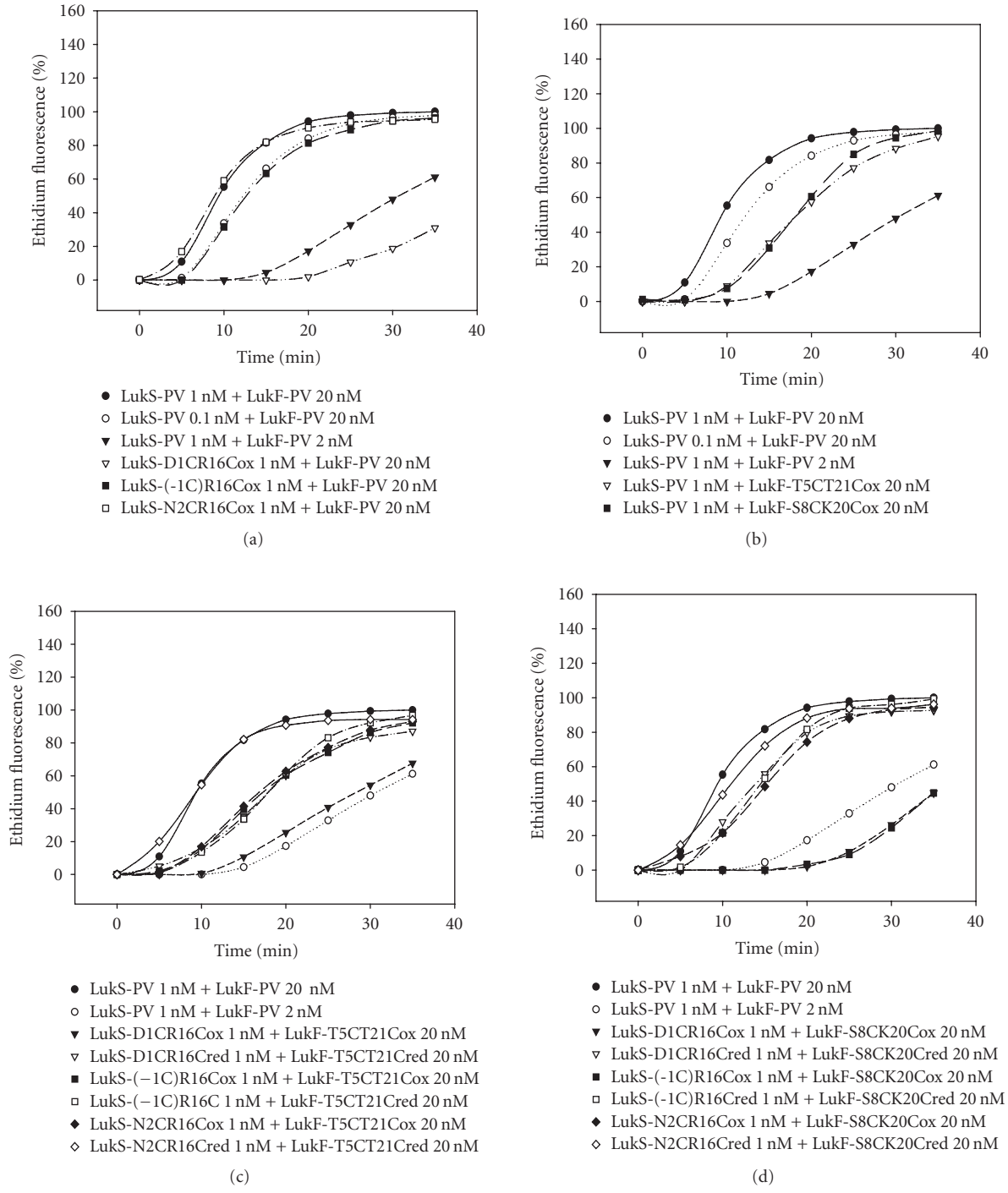

Figure 6: Flow cytometry evaluation of ethidium entry into human PMNs for different combinations of purified WT S and F proteins and their oxidized or reduced double mutants. (a) Oxidized LukS-PV mutants were first tested with WT LukF-PV. (b) Oxidized LukF-PV mutants were tested with WT LukS-PV. (c) Oxidized or reduced LukS-PV double mutants were tested with LukF-PV S8C-K20C. (d) Oxidized or reduced LukS-PV double mutants were tested with LukF-PV T5C-T21C.

identify oligomers species provided that samples were boiled (Figure 8, lanes 7–11), whether saponin treatment was carried out at 4°C or 23°C. In fact, the Schiff reaction promoted by glutaraldehyde is not stable in aqueous solution, but cross-linking certainly occurs in our assays through the Michael addition reaction onto amine groups ($R\text{-}NH_2$). Considering the excess of proteins in lysates, the observed oligomers are assumed as preformed oligomers, since the cross-linking reaction cannot be considered to be specific of the PVL proteins. This addition reaction was stopped by ethanolamine

Table 2: Times (min) to reach (a) 5%, (b) 50%, and (c) 100% of the entry of ethidium into cells by pores formed by combinations of PVL (taken as reference) and its mutants.

	LukF 40 nM	LukF 2 nM	LukF-T5C-T21C	LukF-S8C-K20C
LukS 1 nM	4[(a)] 9.6[(b)] 25[(c)]	15[(a)] 31[(b)] 48[(c)]	9.6[(a)] 18.5[(b)] 35[(c)]	9.6[(a)] 18.5[(b)] 35[(c)]
LukS 0.1 nM	6[(a)] 12.5 35	n.d.	n.d.	n.d.
LukS-D1C-R16C	22[(a)] 45.5[(b)] 70[(c)]	n.d.	12[(a)] 28[(b)] 45.4[(c)]	22[(a)] 36[(b)] 50.2[(c)]
LukS-(-1C)-R16C	6[(a)] 12.5[(b)] 30[(c)]	n.d.	6.5[(a)] 17[(b)] 40[(c)]	22[(a)] 36[(b)] 48.8[(c)]
LukS-N2C-R16C	2[(a)] 8.6[(b)] 25[(c)]	n.d.	6.5[(a)] 17[(b)] 40[(c)]	3[(a)] 15[(b)] 35[(c)]

introduced in the loading buffer and heating in order to minimize the cross-linking duration. Figure 8, lanes 7 and 8 reveal bands corresponding to any intermediates between monomers and octamers that were recognized by anti-LukS-PV and/or (data not shown) anti-LukF-PV affinity-purified antibodies. In fact, instable oligomers obtained after extraction from membranes with saponin might have been stabilized by using cross-linking via glutaraldehyde. The quantity of oligomers recovered was greater for WT toxin and the most biologically active combination of PVL double mutants (Figure 8, lanes 10 and 11) than for the less active one (Figure 8, lane 9) and remained significant compared to PVL oligomers in solution (Figure 8, lane 3).

4. DISCUSSION

Although staphylococcal α-toxin and bipartite leukotoxins fold in a comparable way, differences exist in the sequences and structures of these two subfamilies of toxins that imply differences in function [30]. Another distinction is in stoichiometry. Indeed, α-toxin is known to form heptamers in target cells [20] and hexamers in some different membranes [31]. Recently, octamers were identified in synthetic bilayers and PMNs membrane by using cross-linking between mutated components of gamma-hemolysin [5, 32]. Moreover, the presence of strictly alternating S and F proteins was recently proven in the case of leukotoxin pores [33]. Considering the sequence alignment of the S and F components of leukotoxins and of α-toxin [23], differences between these proteins are located at the N-termini, at each side of the central domain and in the last fifty C-terminal residues. The significance of these differences with α-toxin is not understood, so far. It has been shown that deleting the first two residues or labelling the N-terminal extremity of α-toxin dramatically reduce its biological activity [34, 35]. It is also noteworthy that leukotoxins oligomers are less stable than those of α-toxin, hampering their crystallization. An investigation using infrared spectroscopy did not give evidence of any significant modification in the β-strands content when passing from the soluble state to the pore formed in planar lipid membranes [4].

In this work, we try to bring out arguments that N-terminal extremities of leukotoxins keeping part of the β-sandwich core during pore formation lead to functional toxins, and that a large unfolding of these extremities is not obvious. Despite the fact that the recombinant expression system used in this study adds an N-terminal octapeptide, the proteins that were produced retain a biological activity comparable to native toxins [24, 25]. Moreover, GST fusions of LukS-PV or LukF-PV also proved their binding efficacy. LukS-PV∼GST + LukF-PV was only from 3 to 5 folds less efficient than the corresponding WT proteins, and the LukS-PV + LukF-PV∼GST was also a bit less effective than the WT couple. The binding of LukF-PV∼GST was affected when tested on its GST fusion counterpart protein and the resulting biological activity significantly decreased, but remained biologically active. Thus, the decrease in binding might be due to steric hindrance produced by the fusion, especially in the case of the GST couple. Despite a higher sensitivity of the Ca^{2+} entry assay, the decrease of Ca^{2+} influx induced by the GST couple correlated with its lower pore-forming activity. It can be assumed, therefore, that the decrease in pore-forming activity results from the reduced binding of LukF-PV∼GST (Figure 2(c)). Taking into account all these features, it becomes less realistic that N-terminal extremities of leukotoxins extensively unfold to interact with residues of adjacent monomers located within the lumen of the pore (see Figure 1). Comparatively, the expressed and purified GST∼ α-toxin has no significant activity against rabbit red blood cells, whereas when GST is

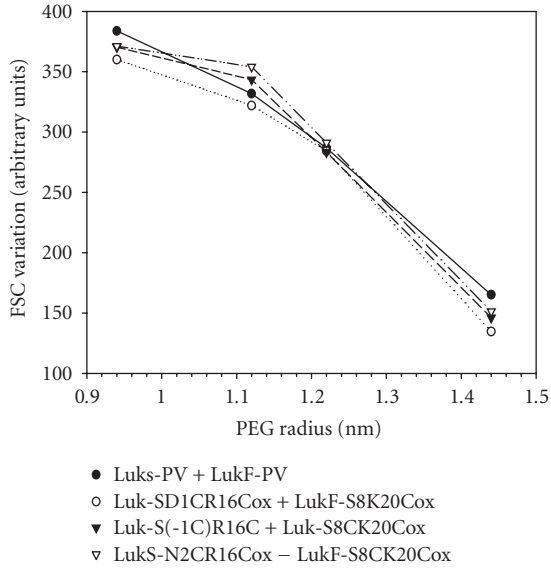

(a)

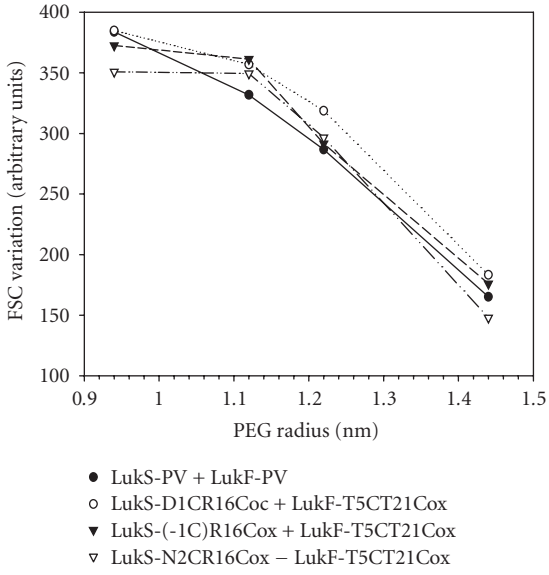

(b)

Figure 7: Determination of the hydrodynamic radius of pores formed by the different combinations of oxidized LukS-PV (20 nM) and LukF-PV (100 nM) mutants 30 minutes after application of toxins to human PMNs. Osmotic protection was assessed by variations of the mean FSC (forward light scatter) value in the presence of polyethylene glycol molecules of different hydrodynamic radii. (a) Oxidized LukS-PV double mutants were tested with LukF-PV S8C-K20Cox. (b) Oxidized LukS-PV double mutants were tested with LukF-PV T5C-T21Cox.

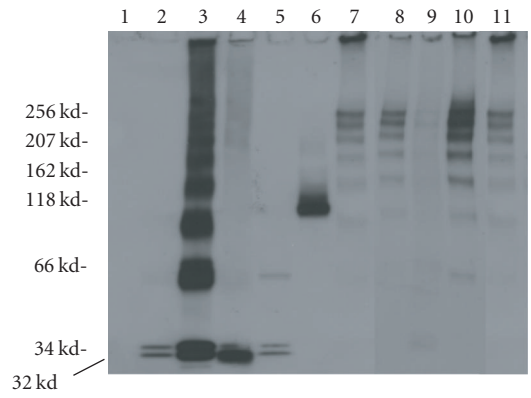

Figure 8: Oligomers formed by PVL and modified toxins. Oligomers were checked in solution or after recovery from treated human PMNs, 3–8% (w/v) SDS-PAGE and immunoblotting with anti-LukS-PV and anti-LukF-PV affinity-purified rabbit antibodies. Lane 1: PMNs only, lane 2: LukS-PV + LukF-PV in solution (4 ng each), lane 3: LukS-PV + LukF-PV (4 ng each/load) treated by 0.3 mM glutaraldehyde, lane 4: LukS-PV + LukF-PV saponin/treated with 3 mM glutaraldehyde. Lanes 5–11: each PVL components (30 ng each/load) was applied on PMNs, lane 5: LukS-PV + LukF-PV saponin treated, lane 6: LukS-PV + LukF-PV saponin- and glutaraldehyde treated without heating at 100°C, lane 7: LukS-PV + LukF-PV saponin at 0°C/glutaraldehyde treated and boiling at 100°C, lanes 8–11: toxins applied on PMNs, saponin treatment at room temperature + 1 mM glutaraldehyde and boiling, lane 8: LukS-PV + LukF-PV, lane 9: LukS-PV-1C-R16C + LukF-PV S8C-K20C, lane 10: LukS-PV N2C-R16C + LukF-PV S8C-K20C, lane 11: LukS-PV + LukF-PV oxidized.

cleaved, the resulted octapeptide-α-toxin shows a lytic activity diminished by more than 10 folds than that of the native α-toxin purified from *S. aureus.* This constitutes a functional difference with the Panton-Valentine leucocidin. Moreover, at least LukF-PV was not sensitive to deletions less than 10 amino acids [36, 37].

In the second approach used in this study, N-terminal extremities of both PVL components were locked to the protein core by disulfide bonds via site-directed mutagenesis. Different locations for cysteine substitution were chosen for each protein. The very first residues and R16 of LukS-PV appeared as good candidates for substitution by cysteines and subsequent bridging. Indeed, although the first two N-terminal residues are absent in the three-dimensional structure of LukS-PV [23], three positions were chosen by analogy with LukF-PV which produced internal disulfide bonds in majority. Thus, formation of homodimers during assisted oxidation could not be responsible for a great decrease in the biological activity of the mutated toxins. Oxidation with 30 mM H_2O_2 could alternatively be preferred to Cu^{2+} oxidation for some mutants, but in any case, excess of oxidant was removed before any biological assays. The binding of oxidized LukS-PV mutants to human PMNs was not affected, but that of LukF-PV S8C-K20C to LukS-PV mutants was diminished from 6 to 15 folds compared to that of WT proteins. This may suggest some modifications in the overall structures and some adverse compatibilities between new structures.

In fact, when combined with LukS-PV, LukF-PV S8C-K20C showed diminishing both in Ca^{2+} induction (> 10 folds) and in pore formation (less than 10 folds), but activities largely decreased for combinations with LukS-PV

D1C-R16C or (-1C)-R16C while they remained significant for the combination with LukS-PV N2C-R16C. Therefore, it can be assumed that LukS-PV N2C-R16C may harbor functionality similar to LukS-PV, and that the decrease in biological activities observed for the couples described above is mainly due to the decrease in binding of LukF-PV S8C-R16C.

In the case of LukF-PV T5C-T21C, the D1C-R16C mutation affects biological activities in any combinations. Nevertheless, LukF-PV T5C-T21C combined with LukS-PV(-1C)-R16C or LukS-PV N2C-R16C induced Ca^{2+} activations and pore formation that only decreased to 3–5 times those of the WT toxins, and thus considering the rigidity introduced into structures confers functions comparable to those of PVL.

To complete our study, we investigated the stoichiometry and the hydrodynamic diameter of the pores. One major difference between the pores formed by leukotoxins compared to those formed by α-toxin is their instability when extracted from target membranes [20, 25]. The use of a dedicated procedure involving the pores excised from cell membranes and the rapid cross-linking with glutaraldehyde allowed us to identify the variety of possible oligomers without a further creation of monomer-monomer interaction, thanks to the 1×100 weight excess of membrane proteins. Hence, a clear indication that octamers are formed by PVL on its target cells has been obtained, whatever the combination of mutated proteins considered. This observation strengthens those works published recently about another leukotoxin onto synthetic membranes [5]. Though our data suggest significant amounts of natural octamers, no indication remains available whether hexamers and heptamers are functional [32]. Osmotic protection of pores using PEG molecules evoked hydrodynamic radii of about 1.2 nm, in agreement with previous data [4, 24, 25], and indicates comparable protections for both WT and mutated toxins.

In conclusion, none of the observations obtained in this work favor a large unfolding and the structural location for interactions with two adjacent protomers along the lumen of the pore for the N-terminal extremities of the Panton-Valentine leucocidin and, probably other bipartite leucotoxin-constituting proteins [24], as it is the case of the related α-toxin (Figure 1(b)) [20]. Recent data have suggested that the N-terminal extremity of α-toxin is probably not exclusively required in the oligomer assembly despite that binding of α-toxin truncates onto membranes remains to be quantified [38]. Other truncates of HlgC and HlgB indicated that the formation of gamma-hemolysin oligomer may support the removing of the first 18 amino acids residues [39]. Slight conformational modification of these extremities during pore formation by bipartite leukotoxins could not be excluded. Constraints via disulfide bonds described in this work support functionality of the modified toxins which has been quantitatively compared. These oligomers clearly promote octameric bipartite pores comparable to WT ones in target cells, even rigidity brought into molecules by these constraints may have lowered some steps in pore-formation process. The next structure determination of assembled S and F proteins may shed new light on the role of their N-termini on the assembly of leukotoxins while they remain domains candidates for substitution by active proteins to challenge their efficacy towards cells.

ACKNOWLEDGMENTS

This work was granted by the "Direction de la Recherche et des Etudes Doctorales" (EA-3432). We thank Gabriella Viero for comments, Eric Martinez and Ben Walsh for English. O. Joubert was supported by grants from a research convention between Provincia Autonoma di Trento (Italy), (Project StaWars) and Université Louis Pasteur, and the "Conseil Régional d'Alsace."

REFERENCES

[1] G. Prévost, "Toxins in *Staphylococcus aureus* pathogenesis," in *Microbial Toxins. Molecular and Cellular Biology*, T. Proft, Ed., pp. 243–284, Horizon Bioscience, Norfolk, UK, 2005.

[2] V. T. Nguyen, Y. Kamio, and H. Higuchi, "Single-molecule imaging of cooperative assembly of γ-hemolysin on erythrocyte membranes," *EMBO Journal*, vol. 22, no. 19, pp. 4968–4979, 2003.

[3] G. Miles, L. Movileanu, and H. Bayley, "Subunit composition of a bi-component toxin: staphylococcal leukocidin forms an octameric transmembrane pore," *Protein Science*, vol. 11, no. 4, pp. 894–902, 2002.

[4] M. Ferreras, F. Höper, M. Dalla Serra, D. A. Colin, G. Prévost, and G. Menestrina, "The interaction of *Staphylococcus aureus* bi-component γ-hemolysins and leucocidins with cells and lipid membranes," *Biochimica et Biophysica Acta (BBA) - Biomembranes*, vol. 1414, no. 1-2, pp. 108–126, 1998.

[5] L. Jayasinghe and H. Bayley, "The leukocidin pore: evidence for an octamer with four LukF subunits and four LukS subunits alternating around a central axis," *Protein Science*, vol. 14, no. 10, pp. 2550–2561, 2005.

[6] G. Prévost, L. Mourey, D. A. Colin, and G. Menestrina, "Staphylococcal pore-forming toxins," in *Current Topics in Microbiology and Immunology: Pore-Forming Toxins*, F. G. V. D. Goot, Ed., pp. 53–83, Springer, Berlin, Germany, 2001.

[7] L. Staali, H. Monteil, and D. A. Colin, "The staphylococcal pore-forming leukotoxins open Ca^{2+} channels in the membrane of human polymorphonuclear neutrophils," *Journal of Membrane Biology*, vol. 162, no. 3, pp. 209–216, 1998.

[8] J.-D. Pédelacq, L. Maveyraud, G. Prévost, et al., "The structure of a *Staphylococcus aureus* leucocidin component (LukF-PV) reveals the fold of the water-soluble species of a family of transmembrane pore-forming toxins," *Structure*, vol. 7, no. 3, pp. 277–287, 1999.

[9] G. Menestrina, M. Dalla Serra, and G. Prévost, "Mode of action of β-barrel pore-forming toxins of the staphylococcal α-hemolysin family," *Toxicon*, vol. 39, no. 11, pp. 1661–1672, 2001.

[10] G. Prévost, B. Cribier, P. Couppié, et al., "Panton-valentine leucocidin and gamma-hemolysin from *Staphylococcus aureus* ATCC 49775 are encoded by distinct genetic loci and have different biological activities," *Infection and Immunity*, vol. 63, no. 10, pp. 4121–4129, 1995.

[11] A. Gravet, M. Rondeau, C. Harf-Monteil, et al., "Predominant *Staphylococcus aureus* isolated from antibiotic-associated diarrhea is clinically relevant and produces enterotoxin A and the bi-component toxin LukE-LukD," *Journal of Clinical Microbiology*, vol. 37, no. 12, pp. 4012–4019, 1999.

[12] M. Dalla Serra, M. Coraiola, G. Viero, et al., "*Staphylococcus aureus* bi-component γ-hemolysins, HlgA, HlgB, and HlgC, can form mixed pores containing all components," *Journal of Chemical Information and Modeling*, vol. 45, no. 6, pp. 1539–1545, 2005.

[13] P. Couppié, B. Cribier, and G. Prévost, "Leukocidin from *Staphylococcus aureus* and cutaneous infections: an epidemiologic study," *Archives of Dermatology*, vol. 130, no. 9, pp. 1208–1209, 1994.

[14] Y. Gillet, B. Issartel, P. Vanhems, et al., "Association between *Staphylococcus aureus* strains carrying gene for Panton-Valentine leukocidin and highly lethal necrotising pneumonia in young immunocompetent patients," *Lancet*, vol. 359, no. 9308, pp. 753–759, 2002.

[15] G. Menestrina, "Ionic channels formed by *Staphylococcus aureus* alpha-toxin: voltage-dependent inhibition by divalent and trivalent cations," *Journal of Membrane Biology*, vol. 90, no. 2, pp. 177–190, 1986.

[16] M. Comai, M. Dalla Serra, M. Coraiola, et al., "Protein engineering modulates the transport properties and ion selectivity of the pores formed by staphylococcal γ-haemolysins in lipid membranes," *Molecular Microbiology*, vol. 44, no. 5, pp. 1251–1267, 2002.

[17] O. V. Krasilnikov, P. G. Merzlyak, L. N. Yuldasheva, C. G. Rodrigues, S. Bhakdi, and A. Valeva, "Electrophysiological evidence for heptameric stoichiometry of ion channels formed by *Staphylococcus aureus* alpha-toxin in planar lipid bilayers," *Molecular Microbiology*, vol. 37, no. 6, pp. 1372–1378, 2000.

[18] A. Valeva, R. Schnabel, I. Walev, F. Boukhallouk, S. Bhakdi, and M. Palmer, "Membrane insertion of the heptameric staphylococcal α-toxin pore. A domino-like structural transition that is allosterically modulated by the target cell membrane," *Journal of Biological Chemistry*, vol. 276, no. 18, pp. 14835–14841, 2001.

[19] J. E. Gouaux, O. Braha, M. R. Hobaugh, et al., "Subunit stoichiometry of staphylococcal α-hemolysin in crystals and on membranes: a heptameric transmembrane pore," *Proceedings of the National Academy of Sciences of the United States of America*, vol. 91, no. 26, pp. 12828–12831, 1994.

[20] L. Song, M. R. Hobaugh, C. Shustak, S. Cheley, H. Bayley, and J. E. Gouaux, "Structure of staphylococcal α-hemolysin, a heptameric transmembrane pore," *Science*, vol. 274, no. 5294, pp. 1859–1866, 1996.

[21] A. Valeva, J. Pongs, S. Bhakdi, and M. Palmer, "Staphylococcal α-toxin: the role of the N-terminus in formation of the heptameric pore—a fluorescence study," *Biochimica et Biophysica Acta (BBA) - Biomembranes*, vol. 1325, no. 2, pp. 281–286, 1997.

[22] R. Olson, H. Nariya, K. Yokota, Y. Kamio, and E. Gouaux, "Crystal structure of staphylococcal lukF delineates conformational changes accompanying formation of a transmembrane channel," *Nature Structural Biology*, vol. 6, no. 2, pp. 134–140, 1999.

[23] V. Guillet, P. Roblin, S. Werner, et al., "Crystal structure of leucotoxin S component: new insight into the staphylococcal β-barrel pore-forming toxins," *Journal of Biological Chemistry*, vol. 279, no. 39, pp. 41028–41037, 2004.

[24] L. Baba Moussa, S. Werner, D. A. Colin, et al., "Discoupling the Ca^{2+}-activation from the pore-forming function of the bi-component Panton-Valentine leucocidin in human PMNs," *FEBS Letters*, vol. 461, no. 3, pp. 280–286, 1999.

[25] S. Werner, D. A. Colin, M. Coraiola, G. Menestrina, H. Monteil, and G. Prévost, "Retrieving biological activity from LukF-PV mutants combined with different S components implies compatibility between the stem domains of these staphylococcal bi-component leucotoxins," *Infection and Immunity*, vol. 70, no. 3, pp. 1310–1318, 2002.

[26] B. Hazes and B. W. Dijkstra, "Model building of disulfide bonds in proteins with known three-dimensional structure," *Protein Engineering*, vol. 2, no. 2, pp. 119–125, 1988.

[27] D. A. Colin, I. Mazurier, S. Sire, and V. Finck-Barbancon, "Interaction of the two components of leukocidin from *Staphylococcus aureus* with human polymorphonuclear leukocyte membranes: sequential binding and subsequent activation," *Infection and Immunity*, vol. 62, no. 8, pp. 3184–3188, 1994.

[28] O. Meunier, A. Falkenrodt, H. Monteil, and D. A. Colin, "Application of flow cytometry in toxinology: pathophysiology of human polymorphonuclear leukocytes damaged by a pore-forming toxin from *Staphylococcus aureus*," *Cytometry*, vol. 21, no. 3, pp. 241–247, 1995.

[29] V. Gauduchon, S. Werner, G. Prévost, H. Monteil, and D. A. Colin, "Flow cytometric determination of Panton-Valentine leucocidin S component binding," *Infection and Immunity*, vol. 69, no. 4, pp. 2390–2395, 2001.

[30] G. Prévost, L. Mourey, D. A. Colin, H. Monteil, M. Dalla Serra, and G. Menestrina, "Alpha-toxin and bêta-barrel pore-forming toxins (leucocidins, alpha-, gamma-, and delta-cytolysins) of *Staphylococcus aureus*," in *The Comprehensive Sourcebook of Bacterial Protein Toxins*, J. E. Alouf and M. R. Popoff, Eds., pp. 588–605, Academic Press, Amsterdam, The Netherlands, 2005.

[31] D. M. Czajkowsky, S. Sheng, and Z. Shao, "Staphylococcal α-hemolysin can form hexamers in phospholipid bilayers," *Journal of Molecular Biology*, vol. 276, no. 2, pp. 325–330, 1998.

[32] O. Joubert, G. Viero, D. Keller, et al., "Engineered covalent leucotoxin heterodimers form functional pores: insights into S-F interactions," *Biochemical Journal*, vol. 396, no. 2, pp. 381–389, 2006.

[33] G. Viero, R. Cunaccia, G. Prévost, et al., "Homologous versus heterologous interactions in the bi-component staphylococcal γ-haemolysin pore," *Biochemical Journal*, vol. 394, no. 1, pp. 217–225, 2006.

[34] B. Walker, M. Krishnasastry, L. Zorn, and H. Bayley, "Assembly of the oligomeric membrane pore-formed by staphylococcal α-hemolysin examined by truncation mutagenesis," *Journal of Biological Chemistry*, vol. 267, no. 30, pp. 21782–21786, 1992.

[35] A. Valeva, A. Weisser, B. Walker, et al., "Molecular architecture of α-toxin pore: a 15-residue sequence lines the transmembrane channel of staphylococcal α-toxin," *EMBO Journal*, vol. 15, no. 8, pp. 1857–1864, 1996.

[36] G. Prévost, "personal communication".

[37] S. Werner, PhD thesis.

[38] L. Jayasinghe, G. Miles, and H. Bayley, "Role of the amino latch of staphylococcal α-hemolysin in pore formation: a cooperative interaction between the N terminus and position 217," *Journal of Biological Chemistry*, vol. 281, no. 4, pp. 2195–2204, 2006.

[39] G. Miles, L. Jayasinghe, and H. Bayley, "Assembly of the bi-component leukocidin pore examined by truncation mutagenesis," *Journal of Biological Chemistry*, vol. 281, no. 4, pp. 2205–2214, 2006.